

DOI: 10.1002/adma.200703236

Alternating the Output of a CdS Nanowire Nanogenerator by a White-Light-Stimulated Optoelectronic Effect**

By Yi-Feng Lin, Jinhui Song, Yong Ding, Shih-Yuan Lu,* and Zhong Lin Wang*

Energy shortage and global warming are two grand challenges to human beings in the 21st century. The development of clean alternative energies and emission control of gases, such as CO₂, have become most-urgent research fields. For the development of clean alternative energies, a wide range of approaches has been explored, including solar cells,^[1] fuel cells,^[2] and thermoelectric devices.^[3] Solar cells, fuel cells, and thermoelectric devices convert optical, chemical, and thermal energies to electrical energy, respectively. Generation of electric energy from conversion of mechanical energy is of great interest owing to its abundance and unique fit for some applications.

Recently, ZnO-nanowire (NW)-array-based piezoelectric nanogenerators have been demonstrated to convert mechanical energy to electricity by utilizing the coupling effect of the semiconducting and piezoelectric properties of ZnO.^[4–6] Further exploration of this piezotronic concept^[7] has led to the development of a wide variety of ZnO-NW-based piezotronic devices, such as piezoelectric field effect transistors,^[8] nanoforce sensors,^[8] and gate diodes.^[9]

More recently, CdS NWs were also successfully demonstrated for piezoelectric nanogenerators.^[10] As another member in the wurtzite family, CdS is a piezoelectric, semiconducting,^[11] and optoelectronic^[12] material with a direct energy band gap of about 2.5 eV^[13] (corresponding to an on-set absorption of 500 nm). A wide range of 1D CdS nanostructures such as NWs,^[14] NW arrays,^[15] nanobelts,^[16] nanotubes,^[17] nanocombs,^[18] and tetrapods,^[19] have been synthesized by wet-chemistry or vapor-phase processes. The photon-induced conduction of 1D CdS nanostructures has also been demonstrated and studied.^[20] A wide variety of 1D CdS nanostructure-based optoelectronic devices, such as photoconductors,^[20] waveguides,^[21] lasers,^[22] logic gates,^[23] field emitters,^[24] and field-effect transistors (FETs)^[25,26] have been developed.

In this Communication, using a single CdS NW as a model system, we have investigated the response of the nanogenerator output when it is subjected to photon excitation. Because the photon has an energy higher than the bandgap of CdS, its excitation not only creates extra charge carriers in the NWs but also modifies the contact of the metal tip with the NWs. The observed piezoelectric output is explained by using the piezotronic process. This experiment demonstrates the triple coupling among piezoelectric, semiconducting, and photonic properties, possibly leading to some unique optopiezotronic devices.

In our experiments, CdS NWs were fabricated by a physical vapor deposition (PVD) process via the vapor–solid (VS) growth mechanism.^[27] Figure 1 shows a transmission electron microscopy (TEM) image of an as-grown CdS NW, which is 400 nm in diameter and several micrometers in length. The selected-area electron diffraction pattern (SAED) reveals the single-crystalline Wurtzite structure of the CdS NW. Furthermore, the axial direction of the NW is $\langle 0001 \rangle$.

Our experiment was based on mechanical manipulation of a single CdS NW by atomic force microscopy (AFM). One end of the CdS NWs was affixed on an insulating silicon substrate by silver paste, and the other end was free to be deflected by the Pt-coated AFM tip (Fig. 2).^[6] Both the topography and the corresponding output voltage (V) images across a load were recorded simultaneously when the AFM tip was scanned across a NW. The topography image reflects the change in normal force perpendicular to the substrate, which shows a bump only when the tip scans over the wire. The output voltage between the conductive tip and the grounded end was continuously monitored as the tip scanned over the wire. The entire experimental process and the output images were captured by video recording, so that we were able to directly visualize the electric generation process. The output data to be presented were obtained from snapshots of the characteristic events observed during the experiments.

To study the effect of light illumination under AFM operation, we first recorded the piezoelectric outputs by deforming a CdS NW in the dark. During a typical AFM tip scan (Fig. 2b), no voltage output signal was observed when the tip touched the stretched side of the CdS NW, while a negative voltage output pulse was received when the tip lifted up and went beyond the central line of the NW to reach the compressed side of the NW, as shown in the surface topography and output voltage plots of Figure 2b. A clear delay in voltage output as compared to the surface topological profile is essential and proves the success of the piezoelectric generation of electricity.

[*] Prof. Z. L. Wang, Y.-F. Lin, J. H. Song, Dr. Y. Ding
School of Materials Science and Engineering
Georgia Institute of Technology
Atlanta, GA 30332-0245 (USA)
E-mail: zhong.wang@mse.gatech.edu
Prof. S.-Y. Lu, Y.-F. Lin
Department of Chemical Engineering
National Tsing Hua University
Hsin-Chu, Taiwan 30013 (ROC)
E-mail: sylu@mx.nthu.edu.tw

[**] This work was supported by the DOE BES (DE-FG02-07ER46394), the NSF (DMS 0706436), and the National Science Council of the Republic of China (Taiwan) under grants NSC-96-2221-E-007-088-MY2 (S.-Y.L.), and NSC 096-2917-I-007-026 (Y.-F.L.).

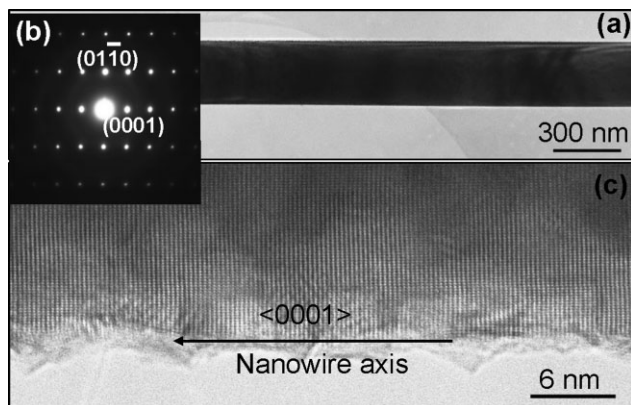


Figure 1. a) Low-magnification transmission electron microscopy (TEM) image, b) corresponding selected-area electron diffraction (SAED) pattern, and c) high-resolution TEM image of the as-grown CdS NW.

If the piezoelectric process was conducted under white light illumination, the electricity generation exhibited a different behavior. The inset of Figure 3 is a snapshot of the in-situ video image taken when the experiment was carried out under white light illumination, clearly showing the NW deflection caused by the scan of the Pt coated AFM tip. Only a positive voltage output of about 2 mV was observed (Fig. 3). Surprisingly, the positive voltage developed when the tip touched the stretched side of the CdS NWs, and there was no negative voltage output even when the tip reached the compressed side of the NW, as otherwise expected for the scan under dark.

To understand the phenomena observed in Figure 3, the transport properties of the CdS NWs were characterized under dark and white light illumination conditions, respectively. To mimic the processes of the piezoelectronic measurements, a single CdS NW was laid alone on an insulated silicon substrate. One end of the NW was fixed with silver paste, and the other was made contacted with a Au-coated tungsten tip, as depicted in Figure 4a. The electron affinity of n-type CdS is 4.8 eV,^[28] while the work functions (ϕ) of Au, Pt, and Ag are about

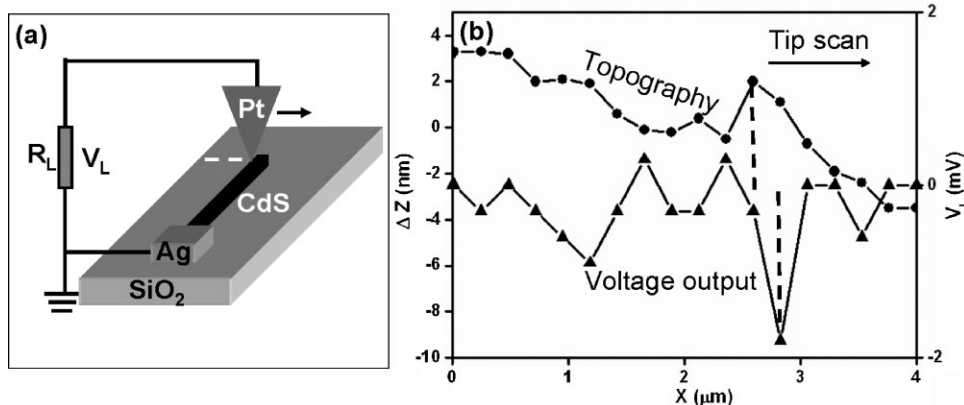


Figure 2. a) Experimental setup for piezoelectric measurements with an AFM instrument. b) Surface topography and voltage output plots of the CdS NWs when the free end was scanned with a Pt-coated AFM tip in the dark. A negative voltage peak was observed when the tip reached the compressed side of the CdS NW.

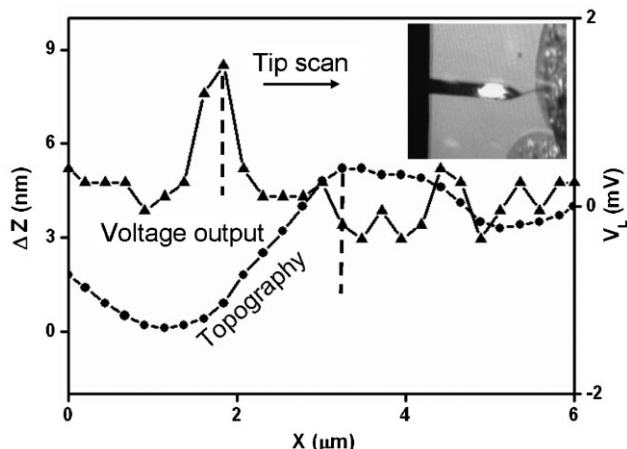


Figure 3. In-situ observation of the piezoelectric measurement process under white light illumination. The inset is a snapshot of the optical image of the AFM tip used to deflect the NWs. A positive voltage signal was observed when the tip touched the stretched side of the CdS NW.

5.25,^[29] 6.1,^[4] and 4.2 eV,^[4] respectively. A Schottky barrier should be established at the contact interfaces of both Au/CdS and Pt/CdS, and an Ohmic contact at the Ag/CdS interface.

The I - V curve measured in the dark confirmed the formation of a typical Schottky contact at the Au-CdS interface. On the other hand, the I - V curve measured under white light illumination deviated from the typical Schottky contact behavior. In the forward-biased region, because of the generation of photocurrent, the conductance of the CdS NW was improved more than 100-fold over that of the scan in the dark case. As for the reverse-biased region, two different characteristics can be identified. The usual Schottky contact behavior remains for $-1.5 < V_e < 0$ V, while an Ohmic contact behavior starts to develop at $V_e < -1.5$ V. This indicates that the Schottky barrier can be broken when the magnitude of the local potential is greater than ca. 1.5 V under white light illumination. Note that white light can generate electron-hole pairs in the CdS NW, and thus increase the carrier density in the NW.^[20] White light is also able to enhance the conductance of CdS and realign the relative energy levels between the CdS NW and Au electrode, leading to a reduced Schottky barrier height. The lowering of Schottky barrier height not only reduces the rectifying effect,^[30] resulting in barrier breakthrough at $V_e < -1.5$ V as shown in Figure 4b, but also weakens the potential preserving capability during the charge accumulation and release process when bending a CdS NW.^[30,31] Consequently, a

increase the carrier density in the NW.^[20] White light is also able to enhance the conductance of CdS and realign the relative energy levels between the CdS NW and Au electrode, leading to a reduced Schottky barrier height. The lowering of Schottky barrier height not only reduces the rectifying effect,^[30] resulting in barrier breakthrough at $V_e < -1.5$ V as shown in Figure 4b, but also weakens the potential preserving capability during the charge accumulation and release process when bending a CdS NW.^[30,31] Consequently, a

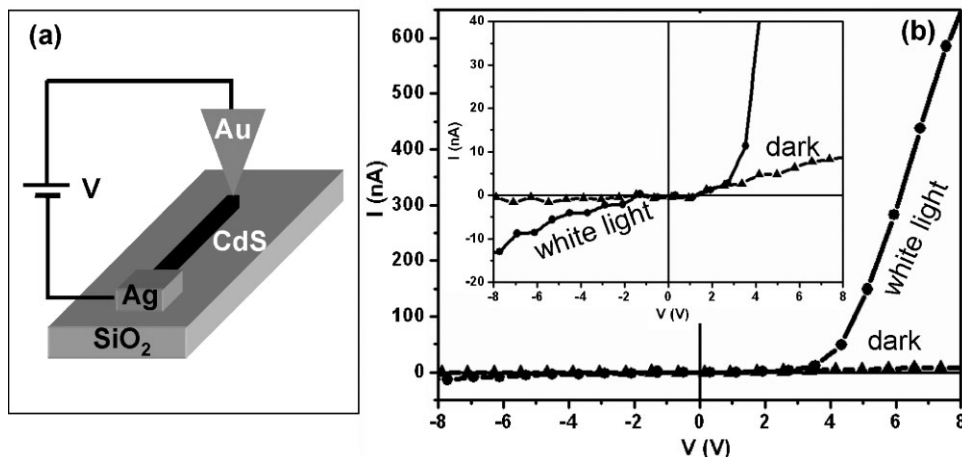


Figure 4. a) Experimental setup for the transport measurement for the CdS NW. The silver paste and Au-coated tungsten tip were used to fix the two ends of the CdS NW and served as the electrodes. b) I - V characteristics of the CdS NW in the dark and under white light illumination, respectively. Inset is the enlarged I - V curve for current values from -20 to 40 nA.

current can be established from the CdS NW to the grounded end by breaking through the height-reduced Schottky barrier, giving rise to the positive voltage pulse during the potential preserving stage when the AFM tip touched the stretched side of the CdS NW.

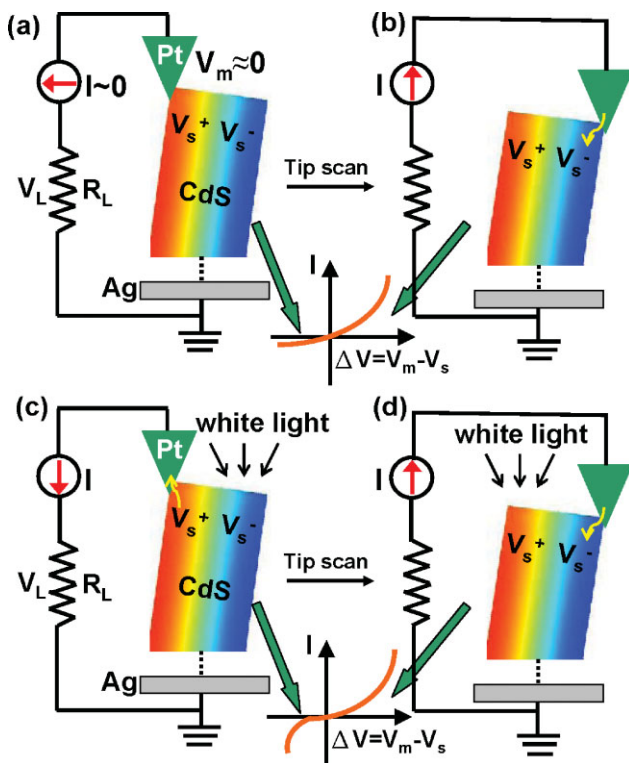


Figure 5. Proposed models for piezoelectric potential generation from CdS NW deflected with a Pt-coated AFM tip. a) and b) in the dark, c) and d) under white light illumination (see text).

We propose here a model, as illustrated in Figure 5, to explain the mechanism behind the two different phenomena we observed with and without white light illumination. First of all, let us examine the scan in the dark case. For this case, the mechanism proposed previously for the ZnO NW based nanogenerators applies.^[6] Briefly, as the Pt-coated AFM tip started to deflect the NW, a positive potential ($V_s^+ > 0$) was produced at the stretched side of the NW while a negative potential ($V_s^- < 0$) was induced at the compressed side.^[4,6] The potential of the tip was near zero, $V_m = 0$, since it was grounded. No voltage signals were observed at this stage because of the presence of the reverse-biased

Schottky barrier between the tip and the stretched side of the n-type CdS NW ($\Delta V = V_m - V_s^+ < 0$). Figure 5a shows the charge/potential accumulation process as the tip touched the stretched side of the NW. When the tip went beyond the central line of the NW and reached the compressed side of the NW, a negative voltage output of about -2 mV was detected on the external load. At this stage, the Schottky barrier at the tip-CdS contact became forward-biased, giving rise to a positive potential difference between the tip and the compressed side of the n-type CdS NW ($\Delta V = V_m - V_s^- > 0$) and thus the current flow from the tip to NW. Figure 5b illustrates how the charge/potential was released from the NW. This charge accumulation and release process can also be clearly seen from the composite plot of the surface topography and voltage output shown in Figure 2b.

For the case of white-light illumination, there are two important points to be noted. First, the height of Schottky barrier is significantly reduced under white-light illumination as discussed above. Second, the magnitude of the piezoelectric potential build-up is proportional to the degree of bending of the NW.^[31] When the tip just started to deflect the NW, the magnitude of deflection was too small to build up a local piezoelectric potential V_s^+ large enough to overcome the height-reduced reverse-biased Schottky barrier. Consequently, no current was allowed to be transported between the tip and the NW, giving no voltage output to the external load at this stage. When the bending of the NW continued, larger deflection resulted in larger local piezoelectric potential V_s^+ to a point that was large enough to break through the barrier with reduced height to allow the current to flow through, resulting in a positive voltage output. If this charge-release process was complete no residual charge would remain, thus, no voltage would be output even when the tip touched the compressed side of the NW. This is the reason that only one

positive voltage peak was observed in most of the cases. If there were residual charges left, a negative peak would be observed when the tip reached the compressed side of the NW, which was observed occasionally. In such a case, the contact time between the tip and the NW might be too short and the NW conductivity might be too low to allow a complete neutralization of the piezoelectric charge/potential generated at the stretched side.

In summary, we have investigated the response of a single CdS-nanowires-based nanogenerator to the excitation of visible light. White light reduces the height of the Schottky barrier existing at the tip/NW contact, leading to possible barrier breakthrough and contact mode change from Schottky to quasi-Ohmic. As a result, a positive voltage output was received when the tip contacted the stretched side of the NW. This is different from the result obtained when there is no light. This study shows the effectiveness of using light to tune the output of the nanogenerator. This work demonstrates the triple coupling among semiconducting, piezoelectric, and optoelectric properties, which may be useful for designing new optopiezotronic devices.^[7]

Experimental

Synthesis of CdS NWs via VS Growth Mechanism: CdS NWs were grown in a PVD process via the VS growth mechanism. CdS powders and Si(111) were used as the CdS source and collecting substrate, respectively. The temperature and pressure of the deposition chamber were set at 950 °C and 160 Torr (1 Torr = 1.333×10^2 Pa), respectively. Nitrogen gas of 100 sccm was used to carry the CdS vapors to the downstream of the growth chamber for deposition. The deposition was run for 60 min.

Morphology and Structure Characterization: The as-prepared CdS NWs were characterized by TEM (JEOL-4000EX at 400 kV).

Opto-Piezoelectric Measurements of a Single CdS NW: A single CdS NW prepared from the PVD process was picked out and put on the insulated silicon substrate. One end of the CdS NW was fixed on the insulated silicon substrate using silver paste that was electrically grounded, while the other end of the CdS NW was left free and deflected consecutively using a conducting Pt-coated silicon tip of an atomic force microscope (model MFP-3 from Asylum Research) to perform the piezoelectric measurements (as shown in Fig. 2a). The piezoelectric and optopiezoelectric measurements of the single CdS NW were conducted in the dark and under white light illumination, respectively. The cantilever of the AFM had a spring constant of 1 N m^{-1} . In contact mode, a constant normal force of 5 nN and a scanning speed of $65.93 \mu\text{m s}^{-1}$ were maintained between the tip and the CdS NW. A resistor R_L of 500 M Ω was mounted between the silver paste fixed end of the CdS NW and the AFM tip, and the output signal was measured by a voltage drop across the resistor in reference to the grounded end. No external voltage was applied during the experiment periods.

Transport Measurement of a Single CdS NW: The manner in which we conducted the transport measurements of the NW mimicked that of

the piezoelectric measurements of the NW. A single CdS NW was placed on the insulated silicon substrate. One end of the NW was fixed with silver paste, while the other end of the NW was made in contact with the Au-coated tungsten tip, as shown in Figure 4a. The externally applied voltage was swapped from -8 to 8 V. The measurements were carried out both in the dark and under white light illumination.

Received: December 30, 2007

Revised: January 16, 2008

Published online: July 4, 2008

- [1] M. Law, L. E. Greece, J. C. Johnson, R. Saykally, P. Yang, *Nat. Mater.* **2005**, *4*, 455.
- [2] J. Malzbender, R. W. Steinbrech, *J. Power Sources* **2007**, *173*, 60.
- [3] J. Yang, T. Caillat, *MRS Bull.* **2006**, *31*, 224.
- [4] Z. L. Wang, J. Song, *Science* **2006**, *312*, 242.
- [5] X. Wang, J. Song, J. Liu, Z. L. Wang, *Science* **2007**, *316*, 102.
- [6] J. Song, J. Zhou, Z. L. Wang, *Nano Lett.* **2006**, *6*, 1656.
- [7] Z. L. Wang, *Adv. Mater.* **2007**, *19*, 889.
- [8] X. Wang, J. Zhou, J. Song, J. Liu, N. Xu, Z. L. Wang, *Nano Lett.* **2006**, *6*, 2768.
- [9] J. H. He, C. L. Hsin, J. Liu, L. J. Chen, Z. L. Wang, *Adv. Mater.* **2007**, *19*, 781.
- [10] Y. F. Lin, J. Song, Y. Ding, Z. L. Wang, *Appl. Phys. Lett.* **2008**, *92*, 022105.
- [11] A. R. Hutson, *Phys. Rev. Lett.* **1960**, *4*, 505.
- [12] Q. H. Li, T. Gao, T. H. Wang, *Appl. Phys. Lett.* **2005**, *86*, 193109.
- [13] Y. J. Hsu, S. Y. Lu, Y. F. Lin, *Adv. Funct. Mater.* **2005**, *15*, 1350.
- [14] Y. J. Hsu, S. Y. Lu, *Langmuir* **2004**, *20*, 23.
- [15] Y. F. Lin, Y. J. Hsu, S. Y. Lu, S. C. Kung, *Chem. Commun.* **2006**, 2391.
- [16] J. Zhang, F. Jiang, L. Zhang, *J. Phys. Chem. B* **2004**, *108*, 7002.
- [17] X.-P. Shen, A.-H. Yuan, F. Wang, J.-M. Hong, Z. Xu, *Solid State Commun.* **2005**, *133*, 19.
- [18] J. Ge, Y. Li, *Adv. Funct. Mater.* **2004**, *14*, 157.
- [19] M. Chen, Y. Xie, J. Lu, Y. Xiong, S. Zhang, Y. Qian, X. Liu, *J. Mater. Chem.* **2002**, *12*, 748.
- [20] T. Gao, Q. H. Li, T. H. Wang, *Appl. Phys. Lett.* **2005**, *86*, 173105.
- [21] R. Agarwal, C. J. Barrelet, C. M. Lieber, *Nano Lett.* **2005**, *5*, 917.
- [22] B. Cao, Y. Jiang, C. Wang, W. Wang, L. Wang, M. Niu, W. Zhang, Y. Li, S. T. Lee, *Adv. Funct. Mater.* **2007**, *17*, 1501.
- [23] R. M. Ma, L. Dai, H. B. Huo, W. J. Xu, G. G. Qin, *Nano Lett.* **2007**, *7*, 3300.
- [24] Y. F. Lin, Y. J. Hsu, S. Y. Lu, K. T. Chen, T. Y. Tseng, *J. Phys. Chem. C* **2007**, *111*, 13418.
- [25] R. M. Ma, L. Dai, G. G. Qin, *Nano Lett.* **2007**, *7*, 868.
- [26] R. M. Ma, L. Dai, G. G. Qin, *Appl. Phys. Lett.* **2007**, *90*, 093109.
- [27] Y. Xia, P. Yang, Y. Sun, Y. Wu, B. Mayer, B. Gates, Y. Yin, F. Kim, H. Yan, *Adv. Mater.* **2003**, *15*, 353.
- [28] R. K. Swank, *Phys. Rev.* **1967**, *153*, 844.
- [29] P. C. Rusu, G. Brocks, *J. Phys. Chem. B* **2006**, *110*, 22628.
- [30] J. Liu, P. Fei, J. Song, X. Wang, C. Lao, R. Tummala, Z. L. Wang, *Nano Lett.* **2008**, *8*, 328.
- [31] J. Song, X. Wang, J. Liu, H. Liu, Y. Li, Z. L. Wang, *Nano Lett.* **2008**, *8*, 203.